

# ORCHID: Streaming Threat Detection over Versioned Provenance Graphs

Akul Goyal  
Computer Science  
University of Illinois at  
Urbana-Champaign  
akulg2@illinois.edu

Jason Liu  
Computer Science  
University of Illinois at  
Urbana-Champaign  
jdliu2@illinois.edu

Gang Wang  
Computer Science  
University of Illinois at  
Urbana-Champaign  
gangw@illinois.edu

Adam Bates  
Computer Science  
University of Illinois at  
Urbana-Champaign  
batesa@illinois.edu

**Abstract**—While Endpoint Detection and Response (EDR) are able to efficiently monitor threats by comparing static rules to the event stream, their inability to incorporate past system context leads to high rates of false alarms. Recent work has demonstrated Provenance-based Intrusion Detection Systems (Prov-IDS) that can examine the causal relationships between abnormal behaviors to improve threat classification. However, employing these Prov-IDS in practical settings remains difficult – state-of-the-art neural network based systems are only fast in a fully offline deployment model that increases attacker dwell time, while simultaneously using simplified and less accurate provenance graphs to reduce memory consumption. Thus, today’s Prov-IDS cannot operate effectively in the real-time streaming setting required for commercial EDR viability.

This work presents the design and implementation of ORCHID, a novel Prov-IDS that performs fine-grained detection of process-level threats over a real time event stream. ORCHID takes advantage of the unique immutable properties of a versioned provenance graphs to iteratively embed the entire graph in a sequential RNN model while only consuming a fraction of the computation and memory costs. We evaluate ORCHID on four public datasets, including DARPA TC, to show that ORCHID can provide competitive classification performance while eliminating detection lag and reducing memory consumption by two orders of magnitude.

## 1. Introduction

Effective logging plays a crucial role in defending against malicious behavior. Most of today’s cyber-attacks can forensically be captured through a combination of multiple log streams. However, the sheer volume of logs generated poses a significant challenge for organizations, demanding substantial computational and memory resources for proper analysis and storage. For instance, even in a small data center, daily host logs can quickly accumulate hundreds of gigabytes of data [1]. Moreover, reliant defense against modern cyber-attacks necessitates security tools to offer real-time detection capabilities without excessively burdening the underlying system resources. Consequently, current commercial security solutions meet these demands by adopting a strategy of lightweight analysis, using pat-

tern matching based on pre-defined rules, implemented on coarse-grained logging systems like Sysmon [2] or Carbon Black [3], in place of the heavier analysis of the finer-grained logging systems such as Linux AuditD [4]. While this approach seeks to balance performance and system scrutiny, it also introduces a trade-off that exposes organizations to undetected attack steps when certain logs are not collected and analyzed. As such, finding the optimal compromise between tool efficiency and the thoroughness of log data remains a critical challenge in fortifying cyber defenses.

Data provenance has emerged as a potential contender to address some of these challenges, utilizing the low-level system calls to learn malicious behaviors and cutting down on false positives while still identifying malicious behavior. Provenance research timestamps system calls within audit logs to create causal dependency graphs that correctly model system activity. The graphical structure maintains the causal relationship between events regardless of how temporally apart they occur. Much of the current Provenance-based Intrusion Detection Systems (Prov-IDS) research has primarily focused on analyzing these graphical structures to identify the occurrence of anomalous substructures accurately. Initial research [5]–[9] focused on building lightweight systems that provided global classification over the entire graph. However, recent work [10], [11] has shown that these systems were vulnerable to mimicry attacks that allowed the attacker to evade detection. More modern solutions [12] have adapted to the mimicry problem by focusing on more sophisticated models that provide finer-grained classification (node-level, edge-level). Nonetheless, these solutions have occurred at the expense of creating memory and computationally intensive systems – analyzing a canonical fully versioned provenance graph calls for **143.7 GB** of memory. These Prov-IDS rely on static audit logs requiring them to be deployed at specific “checkpoints” to transform the input logs into an in-memory graphical format, which the Prov-IDS then uses to train, embed, and detect for abnormal activity.

In this paper, we introduce ORCHID (Online Root Cause Host Intrusion Detection System), a stream-based node-classifying Prov-IDS with a low memory footprint and accurate identification of attacker behavior. The foundation

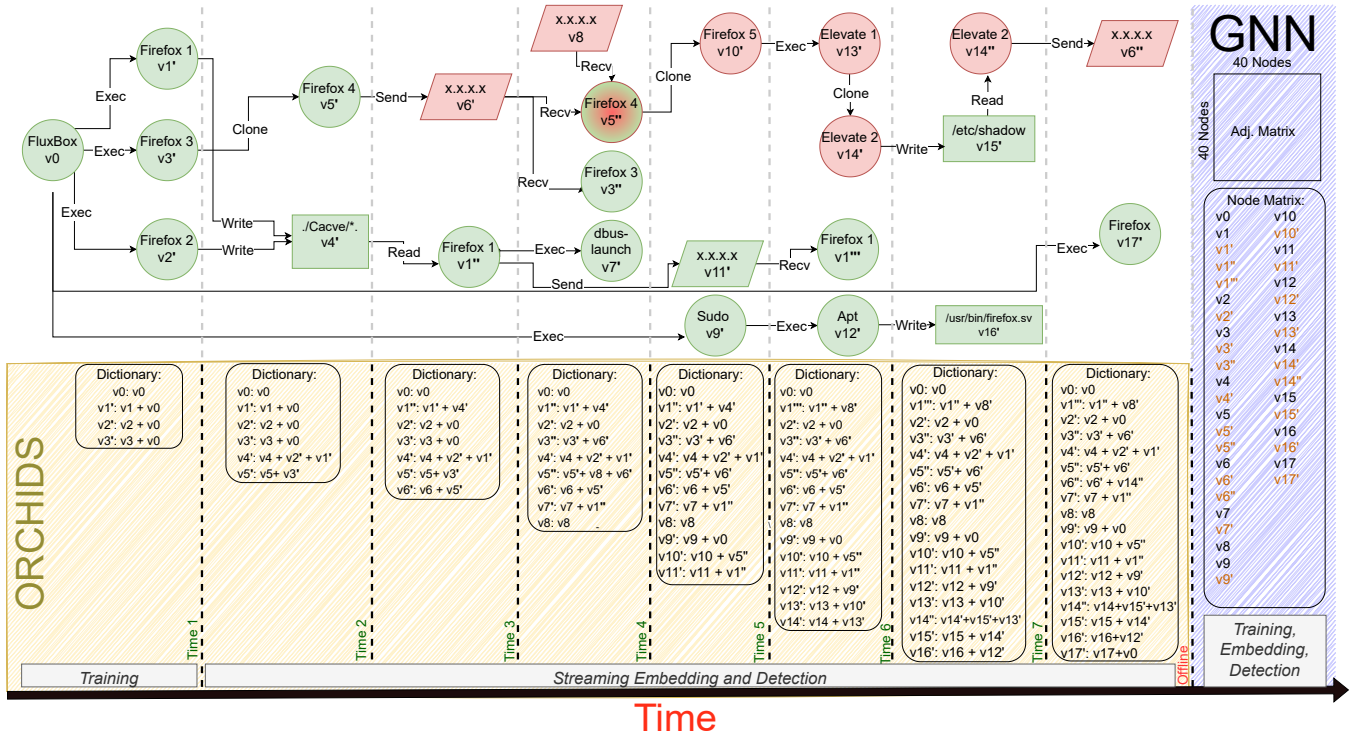


Figure 1: Overview of the ORCHID architecture, as demonstrated on an example provenance graph. Green and red nodes represent benign and attack entities, respectively. To create a more precise and acyclic provenance graph, entities are *versioned* in the graph as they are updated, e.g.,  $h1'$  is a new version of  $h1$ . In a GNN, the entire graph including testing data must be collected before training begins. In contrast, ORCHID continuously embeds and classifies new events as they occur following a preliminary training period. Times 1-7 demonstrate how ORCHID’s *streaming* dictionary has evolved at discrete points in the timeseries. By only maintaining state on the current version of system entities, ORCHID is able to maintain a smaller memory footprint, as can be seen by comparing the dimensions of its dictionary to the GNN’s matrices.

for ORCHID resides in using a sequential-based machine learning model to model audit logs while adhering to their graphical format. Unlike its predecessors, ORCHID does not generate and store the entire provenance graph in memory. Instead, ORCHID keeps an  $L$ -dimensional embedding for each system entity that encodes its full history on the system. This significantly reduces memory usage compared to prior approaches, while the embeddings contain more information than their predecessors. Additionally, to overcome the long-standing challenges with sequential models of capturing long-term dependencies, ORCHID utilizes root causes to introduce additional context to the sequential model, allowing for more accurate embeddings.

In our comprehensive evaluation of ORCHID, we compare ORCHID to GNN-based architectures used in state-of-the-art Prov-IDS, including an adaption of GNNs for streaming settings. We find that ORCHID is nearly as effective at threat classification as a GNN in an offline model, but significantly more effective than GNNs in an online streaming model (e.g., 0.91 vs. 0.73 AUC on DARPA TC3 Theia [13]). We go on to demonstrate that ORCHID has a dramatically lower memory footprint than GNNs (2.7 GB vs. 143.7 GB on DARPA TC3 Trace [13]). Finally, we demonstrate that

while ORCHID is able to embed and classify new events in near real time (0.002 seconds per event), *in practice offline GNN models may experience detection lag of 18 to 42 hours.*

The rest of this paper is organized as follows. In Section 2, we motivate our approach and consider the limitations of prior work. Section 3 presents the threat model that guides our design. We present the design of ORCHID in Section 4. Section 5 presents our experiments and performance results. We revisit related work in Section 6, consider limitations of our approach in Section 7, and conclude in Section 8.

## 2. Motivation

To illustrate the challenges faced Provenance-based Intrusion Detection System (Prov-IDS), we draw upon a realistic example of an Advanced Persistent Threat (APT) attack observed in the DARPA Transparent Computing Attack Engagement 5. The attacker starts off by strategically placing a malicious ad server on a trusted website, specifically `www.allstate.com`, and waiting for a potential victim with a vulnerable Firefox browser to visit. Upon connection, the attacker installs a Drakon implant in the memory of the victim’s Firefox process resulting in the exploited Firefox

establishing a connection back to the attacker’s server with the IP address 189.141.204.211 ready to receive commands. With control of the process, the attacker escalates their privileges on the system by capitalizing on a previously installed driver named “BinFmt Elevate.” This driver allows the attacker to execute an Elevate process with elevated root access to the victim system. The attacker uses the higher privilege process to access sensitive data `etc/shadow` and subsequently exfiltrate this data back to their server. During the attack, the victim performs benign activities, including updating Firefox.

A causal graph of the attack is depicted in Figure 1, with red nodes indicating malicious behavior and green nodes representing legitimate activity. The W3C definition of a provenance graph [14] states a causal graph must be directed and acyclic. We achieve this by employing *graph versioning* [15] wherein a new node is created for a system entity when it *receives* a new information flow and the its “old” node becomes *locked*.

New edges are appended only to unlocked nodes making locked portions of the graph *immutable*. Figure 6 (Appendix) visualizes an audit log and its corresponding versioned provenance graph.

## 2.1. Key Limitations of Prior Work

In Figure 1, the attacker’s behavior appears noticeably distinct from the normal activities; however, in practice provenance-based anomaly detectors face many challenges. To demonstrate, we consider an exemplar Graph Neural Network (GNN) based Prov-IDS architecture used by systems like ShadeWatcher [12] and R-CAID [16]. These system represent the state-of-the-art in terms of their ability to perform fine-grained entity-level detection in a provenance graph; coarser-grained graph-level Prov-IDS are discussed in Section 7. Note the right hand side of Figure 1 visualizes a GNN’s internal representation of the Drakon attack.

**Memory Overhead.** Provenance graphs quickly grow massively in size, e.g., 130GB for a single day on a single machine [17]. This necessitates careful design when choosing how to store and analyze provenance graph. Ideally, as shown in Figure 1, the GNN would track state for all 40 nodes within the versioned provenance graph, despite only 17 system entities existing. However, to be more memory efficient, prior work reduces memory and analysis costs by using a simplified causal graph that contains cycles.<sup>1</sup> Unfortunately, this compromise sacrifices temporal ordering and event occurrence information that may be crucial to detection. For example, benign `Firefox 1` uses an exec call to launch `dbus-launch` *before* connecting to an IP address. Conversely, in the attack subgraph, `Firefox 4` executes the malicious `Elevate` process *after* connecting to the malicious IP address. Loss of temporal information renders both activities almost identical, making it harder for Prov-IDS to detect.

1. The simplified GNN state model used in prior work would contain single node per system entity and the adjacency matrix would allow cycles.

**Detection Lag.** Minimizing an attacker “dwell time” [18] by reducing the time to detection is an essential goal for any threat detection system. However, GNN-based architectures assume access to a *static graph* which provides access to all training and testing data at once. This means GNN-based Prov-IDS are required to operate in a *fully offline* model where training cannot begin until *after* the desired inference period has already occurred. This is depicted in Figure 1, where the time axis shows that the GNN does not begin training until after the attack has concluded. This approach is a boon to the attacker, guaranteeing them additional dwell time equivalent to the combined lengths of the GNN’s costly training and inference periods.

## 2.2. Our Approach

We have shown that effective Prov-IDS design requires operating on *lossless* provenance graphs while maintaining the memory and computational efficiency for *real-time analysis* of the event stream. This requires rethinking the underlying architecture to construct the graph and facilitate the embedding and detection process. ORCHID uses an sequential-based neural network (SNN) to learn an embedding function on a preliminary portion of the provenance graph (Time 1 in Figure 1). It then performs real-time analysis of the audit event stream. As new events occur, ORCHID efficiently embeds and tests the current version for each system entity. Because ORCHID maintains an entry only for the most recent version of each system entity and no edge state, the complexity of its state model is dramatically streamlined compared to GNN architectures.

To better understand why ORCHID can effectively and securely operate under a simpler state model, we will utilize the attack in Figure 1. Consider at Time 7 the introduction of malicious `Elevate 2` process (or  $v14'$ ) whose representation is defined as  $v14' = v14 + v13'$ , where  $v14$  is `Elevate 2` feature vector and  $v13'$  is a recursive embedding of event history including the vulnerable `Firefox 4` process getting exploited by the attacker. So at Time 8, when `Elevate 2` reads from `/etc/shadow`, the inherent abnormality of information flow between a highly sensitive data source and a node whose history includes an outside IP address ( $v6, v8$ ) is represented in the summation of  $v15$  and  $v14'$ . As a result, the  $L$ -dimensional embedding  $v14''$  should appear as an outlier when compared against a model capturing normal behavior. This recurrent structure employed by ORCHID allows for simple computation to create  $v14''$  which then fully capture `Elevate 2`’s history without requiring previous versions ( $v14', v14$ ). This reduces the computational and memory costs associated with the detection system while still allowing it to remain accurate. In the following sections we will detail exactly how the architecture of ORCHID allows it effectively stream over the incoming event log.

Diagram	Syscall
	Clone/Fork/Exec
	Write
	Read
	Send
	Recv

TABLE 1: Table visualizing the graphical representation for the 5 different event types ORCHID focuses on.

### 3. Threat Model

In this work, we consider a threat model that is consistent with past work [5]–[9], [12], [19]. We consider an adversary that employs a sophisticated attack strategy, drawing from various techniques described in the MITRE ATT&CK framework [20]. For example, the attacker may engage in mimicry attacks or other forms of masquerading (T1036 [21]), manipulating features of their own artifacts to appear legitimate to security tools. Consistent with prior work, we place the following restrictions on the adversary. We assume the attacker cannot tamper with or turn off mechanisms in the trusted computing base of the system, compromised of the operating system, auditing subsystem, and the Prov-IDS. Beyond these assumptions, we place no further restrictions on the adversary.

### 4. ORCHID Design

In this section, we will detail the design of ORCHID. We will start by introducing notation and background knowledge that we will utilize throughout the rest of the paper. Next, we will detail the foundations of ORCHID and its use of a sequential-based neural network (SNN) to analyze provenance graphs. We will then describe how ORCHID can provide meaningful representations, maintaining a low memory and computational overhead in real-time. Finally, we will explain how ORCHID classifies anomalies and how we trained and tested ORCHID.

#### 4.1. Preliminaries and Background

For a given host system  $S$ , let the audit log  $A$  be a file that continuously records every interaction that utilizes the operating system. Each line  $a_i = (v_i, v_j, r_k, t)$  in  $A$  represents a directed edge defined as a system call ( $r_k$ ) between the source system entity ( $v_s$ ) and the destination system entity ( $v_j$ ) that occurs on the system at time  $t$ . We focus on three different types of system entities (process, file, socket) and five different event types. Table 1 summarizes the system calls and provides a graphical representation - importantly, each pair of system entities and system call is unique such that for any two system calls  $(v_i, v_j, rel_k)$ ,  $(v_j, v_i, rel_l)$ , it is always true that  $rel_k \neq rel_l$ . Intuitively, the direction of each system call defines the flow of information within the system, and the same system call cannot represent two different flows.

**Provenance Graph.** A provenance graph  $G = \langle V, E \rangle$  is a directed acyclic graphical representation of the audit log  $A$  adhering to a strict temporal property [14]. This property ensures that for every node  $v_i \in V$ , all incoming edges  $(v_j, v_i, r_k, t_1), \dots$  occur chronologically prior to any outgoing edges  $(v_i, v_l, r_m, t_2), \dots$ . Previous methods employ a technique known as *versioning* [15] to achieve temporal correctness. For a given vertex  $v_i$ , versioning inserts an identical (same initial feature vector) vertex  $v'_i$  whenever an incoming edge occurs after an outgoing edge. For instance, in Figure 6 of the Appendix, lines 2 and 6 in the audit log have `firefox1` writing and then reading from `/.cache/*`. In a non-versioned graph, this interaction would be a cycle between `firefox1` and `/.cache/*` violating the temporal property of provenance. The cycle is broken by versioning `firefox1'`, resulting in a provenance graph that is both directed and acyclic [14]. Note that once a node ( $v_i$ ) is versioned  $v'_i$ , its initial state ( $v_i$ ) is immutable and unable to be modified within the graph. Finally, a *causal subgraph*  $P(v_d, t)$  is the subgraph resulting from a backward trace from node  $v_d$  to all the roots within  $G$  at timestep  $t$ . In a streaming setting, given graph  $G$  is constantly updated and  $v_d$  has yet to be versioned,  $P(v_d, t)$  at timestep  $t$  can be different from  $P(v_d, p)$  at a later timestep  $p$ .

**Sequence-Based ML and RNN.** Sequential-based machine learning models represent the temporal dynamics and inherent dependencies found between data points to generate accurate embeddings for time series. To illustrate, consider a sequential model  $f$  operating on a data sequence  $s = (s_0, \dots, s_n)$  and its corresponding sequence of feature vectors  $x = (x_0, \dots, x_n)$  where each token  $x_i$  represents a numerical representation of its corresponding element  $s_i$ . During prediction, the sequential model  $f$  takes the input sequence  $x$  and produces an output sequence  $x' = (x'_0, \dots, x'_n)$  where each element  $x'_i$  captures the relationship between  $x_i$  and the other elements in the sequence. Past research has introduced sequential-based neural networks, including recurrent neural networks (RNNs), transformers, convolutional neural networks (CNNs), hidden Markov models (HMMs), and conditional random fields (CRFs).

In our work, we leverage RNNs [22] due to their use of recurrence to capture temporal dependencies. Consider  $f$  to be an RNN; at each step  $t$  within  $x$ ,  $f$  takes in as inputs both the current feature vector  $x_t$  and the hidden state  $h_{t-1}$  from the previous timestep. At timestep  $t$ ,  $h_t = f(x_t, h_{t-1})$  represents the embedding process aggregating the  $L$ -dimensional feature vector  $x_t$  and the previous hidden state  $h_{t-1}$  produce a new hidden state  $h_t$ . The updated hidden state  $h_t$  represents an embedding of the sequence up to timestep  $t$ .

#### 4.2. Key Idea

Consider a dynamic audit log  $A$  where at each timestep  $t$ , a system call  $a_t = (v_i, v_j, r_k, t)$  between the system entities  $v_i$  and  $v_j$  is added.

ORCHID *directly* operates on  $A$  to construct embeddings more specifically, as each event  $a_t = (v_i, v_j, r_k, t)$  occurs,

ORCHID uses a sequential-based neural network  $f$  to generate an embedding using:

$$D[v_j] = f(D[v_j], D[v_i]) \quad (1)$$

where  $D$  is an internal dictionary that maps each vertex to its most up-to-date embedding, and  $f$  is the RNN. This procedure is highly *localized*, where each event  $a_t$  only updates a single dictionary entry, resulting in a constant time operation.

Equation 1 allows for a system entity  $v_j$ 's entire provenance history  $P(v_j, t)$  to be expressed as a single feature vector  $D[v_j]$ .

### 4.3. Vectorizing System Entities

Generating a numerical feature vector for each system entity within the audit log is necessary for RNNs as inputs. To accomplish this, we first represent each system entity in terms of its full system path, which denotes the entity's location on disk. File paths represent files, processes by the path to their binary executable, and sockets by their connecting IP addresses. We use Doc2Vec [23] to generate a  $L$ -dimensional embeddings for each system entity.

### 4.4. Embedding and Detection

To detect and identify abnormal behavior, ORCHID creates a set of benign embeddings representing normal behavior. ORCHID achieves by processing the entire training dataset and generating an  $L$ -dimensional embedding for each system entity.

With this set of training embeddings, ORCHID can detect anomalies in unseen data. For each new edge  $a_t = (v_i, r_k, v_j)$  streamed in, ORCHID generates an  $L$ -dimensional embedding for  $v_j$  using Eqn. 1 that is then compared against the set of training embeddings. The distance between  $v_j$ 's embedding and its closest neighbor determines its anomaly score. If this distance exceeds a pre-defined threshold  $\alpha$ , the ORCHID flags  $v_j$  as anomalous.

### 4.5. Accounting for Long Term Dependencies

Sequential based neural networks have long been recorded [24] to have issues modeling long sequence lengths. To harden ORCHID and allow it to capture long-term dependencies, we propose the introduction of "root-node" embeddings.

Root causes are widely acknowledged as a vital source of information indicating the attacker's origin. Moreover, unlike later attack steps, the attacker cannot manipulate root causes without directly tampering with the log. We incorporate root causes by introducing an additional component called "root embedding." We reflect this component in a modification to the RNN's update function such that:

$$h_i = w * (h_{i-1}) + b * (x_i) + c * \left[ \frac{1}{n} \sum_{i=0}^n \{r_i\} \right] \quad (2)$$

where  $\{r_i\}$  is the set of root nodes associated with element  $i$  in the sequence, and  $c$  is a learnable model weight-optimized to balance the information introduced by root embedding. Root embedding maintains significant relationships over extended distances, invisible to the RNN, thereby enhancing ORCHID's resilience against an active attacker.

## 5. Evaluation

In this section we provide results evaluating ORCHID. For each experiment we wanted to answer the following research questions:

- *RQ1* What are the relative contributions of ORCHID's different components and parameters to classification performance?
- *RQ2* How accurate is ORCHID in identifying anomalous behavior as compared to past approaches?
- *RQ3* What are the performance gains and benefits that are accrued by ORCHID over previous work?

### 5.1. Datasets

To evaluate the performance of ORCHID we use 4 different datasets: StreamSpot, DARPA Transparent Computing Engagement 3 Theia and Trace, and ATLASv2.

StreamSpot. is a multi-graph dataset describing five benign web browsing behaviors (CNN, YouTube, video game, GMail, file download) and one attack behavior (Firefox drive-by-download exploit). Each behavior is automated and repeated 100 times, resulting in 600 total graphs, where each graph is relatively small (50K edges to 700K edges). As stated in Section 4, ORCHID's design intrinsically supports multiple disconnected graphs without issue. So, we combined all the graphs into a single audit log with unique entity identifiers for each graph. We interleave the five benign behaviors and then append all the attack behaviors at the end. We permit ORCHID to train on a single instance of each benign behavior for the preliminary training period. As a result, ORCHID training, validation, and testing split is 1%, 1%, 98% respectively.

DARPA Transparent Computing E3. These datasets consist of system graphs collected from various hosts over a 10-day period, with both benign activity on each host and red team attacks against each host [13]. We make use of the Theia (Ubuntu Linux 12.04), comprised of 21M edges, and Trace (Ubuntu Linux 14.04), comprised of 260M edges. The majority of attacks performed involved exploiting Firefox to run drakon on the victim host. Most attacks were performed towards the end of the 10-day period, but some attacks happened earlier. We restrict the training data to the amount of benign data before the first attack, or about 1 day of data.

ATLASv2. replicates the attack engagements conducted by Alsheel et al. [25] in their evaluation of the ATLAS threat investigation system. It comprises 10 attack chains, including both single-host and two-host attacks, although many of the steps in the chains partially overlap between attacks. A notable limitation of the original ATLAS

dataset was the lack of meaningful benign activity. While the authors did include limited benign activity, it does not follow a realistic usage profile and is insufficient to train one class anomaly detection models. ATLASv2 [26] addresses these limitations through the introduction of a four-day period of benign naturalistic activity generated by human users, followed by a final day in which background activity continues as the attacks occur. We make use of the Microsoft Windows Security Auditing logs from this dataset, with the first day used for preliminary training.

**Ground Truth Labeling.** The absence of a standardized ground truth labeling methodology for intrusion detection, datasets present a notable challenge to the community. Existing datasets employ disparate labeling approaches. Streamspot labels entire logs/graphs as either malicious or benign, the original ATLAS dataset labels only a minority (2-3) of system entities as malicious in each attack chain, while DARPA TC datasets provide qualitative ground truth descriptions but no explicit labeling at all. This lack of uniformity in ground truth labeling raises concerns of both reproducibility and bias in IDS evaluations. To avoid these issues, we make use of the recently released *Recover Every Attack Process* (REAPr) label set [27]. REAPr contains process-level ground truth labels for all of the datasets above using a standardized provenance-based labeling methodology. Marking every process on the path between an attack’s root causes and terminal impacts as malicious, REAPr provides a more comprehensive set of attacker-influenced processes while avoiding the potential for experimenter bias. Details of the REAPr labeling methodology can be found online.<sup>2</sup>

## 5.2. Hyperparameter Tuning (RQ1)

We now explore the relative contributions of different components of the ORCHID framework. We consider six facets of ORCHID: selection of the RNN model, number of model layers, amount of training data, inclusion of root node adaptation, size of the feature vector, and the classification task. To facilitate faster testing of various model parameters, we use the StreamSpot dataset (except where otherwise noted) due to its smaller size. The outcomes of the hyperparameter search are illustrated in Figure 2, wherein each plot presents the Receiver Operating Characteristic (ROC) curve that compares ORCHID’s true and false positive rates under variable classification thresholds.

**RNN Model Comparison.** As we previously demonstrated in Section 4.2, a sequential neural network is best adapted to ORCHID because it can effectively model causal paths given limited information about the underlying sequence. However, as noted in Section 4.5 the SNN suffers from a memory loss issue, which may impede its ability to model longer sequences of attack behaviors effectively. Cho et al.’s Gated Recurrent Units (GRUs) mechanism [28] addresses this limitation of RNNs through a gating mechanism that selectively updates and resets information. Comparing

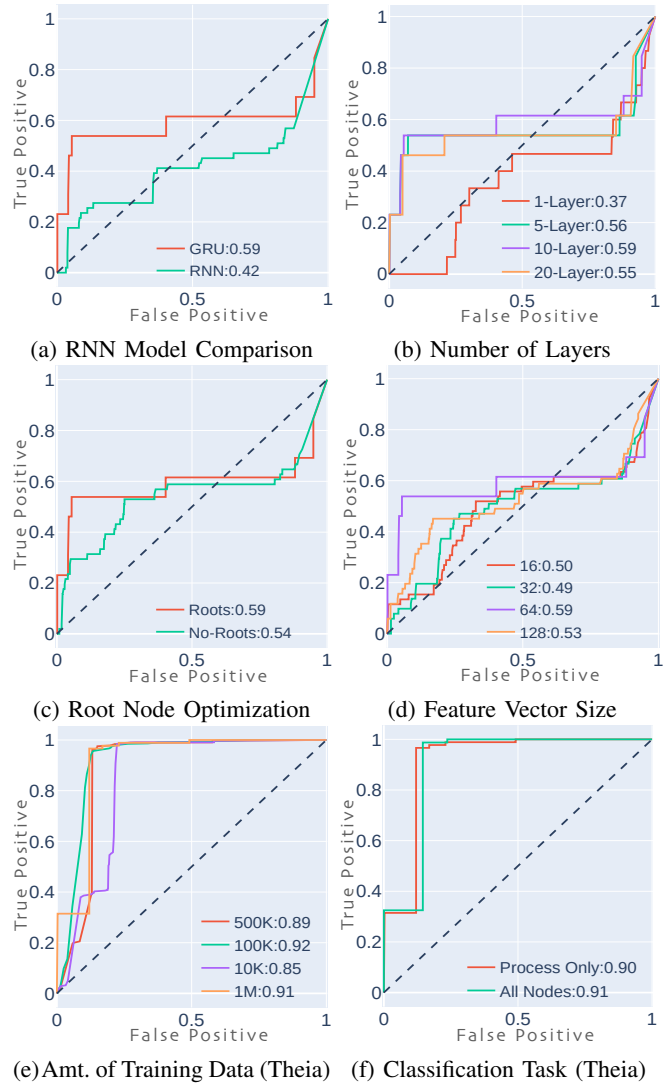


Figure 2: Hyperparameter tuning of ORCHID. Area Under Curve (AUC) for each line is reported in the legend.

the RNN and GRU architectures with all other model parameters constant (Fig. 2a), the GRU outperforms the RNN even on the relatively short-lived Streamspot dataset (0.59 vs. 0.42 AUC). We thus employ GRU as the model backbone for ORCHID. It should be noted that this results in a higher computational demand, which extends training and testing times.

**Number of Layers.** Previous research [29] has highlighted the impact of model size on performance. Continuing with the GRU, we vary the number of model layers (1, 5, 10, 20) in Figure 2b. As anticipated, increasing the number of layers improved classification performance, but concomitantly increases the computational resources required. While the 1-layer GRU performs markedly worse (0.37 AUC), we observe diminishing returns on increased model size between the 5-, 10-, and 20-layer models. We chose a 10-layer GRU for the subsequent experiments.

2. <https://bitbucket.org/sts-lab/reapr-ground-truth>

**Root Node Optimization.** To mitigate RNNs’ difficulty in modeling longer-term dependencies, ORCHID includes an optimization that directly embeds every entity’s root causes alongside its local context (Section 4.5). We compare the performance of ORCHID with and without this optimization in Figure 2c. Including this optimization improves ORCHID’s classification overall (0.59 vs. 0.54 AUC), pronounced at low FPR values. These findings demonstrate that the additional context provided by root causes can help detect additional attack entities that ORCHID might have overlooked.

**Feature Vector Size.** The feature vector that serves as a numerical representation of each system entity is a crucial parameter in ORCHID. While richer feature vectors may better capture underlying data distributions, the inclusion of additional information could also introduce noise. Comparing different vector sizes in Figure 2d, a vector of size 64 achieves the most favorable ROC curve (0.59 AUC). We use this size for the remainder of our experiments.

**Amount of Training Data.** While the size of ORCHID’s preliminary training dataset could play a crucial role in its performance, moving into the streaming phase as quickly as possible is desirable. To determine an appropriate training dataset size, we make use of the larger Theia dataset. Starting with a training dataset of 10K edges, we gradually increased the size to 1M edges, where 1M edges correspond to a single day of logging on the host system. As illustrated in Figure 2e, there is a general trend of improved classification performance as training data increases. We choose to train ORCHID on 1M events (0.91 AUC) in subsequent experiments; this amount is roughly proportional to a full day of activity and is likely to generalize better to other datasets.

**Classification Task.** While ORCHID can classify any system entity in the provenance graph, performance could vary between process entities and data entities like files or sockets. Continuing with the Theia dataset, we compare process-only to all-entity embedding performance in Figure 2f. Surprisingly, we do not observe a meaningful difference between the two tasks, with “All Nodes” classification negligibly outperforming “Process Only” (0.91 vs 0.90 AUC).

### 5.3. Classification Results (RQ2)

We now evaluate the classification performance of ORCHID. Recall every process on the attack path is marked as malicious, meaning ORCHID is being evaluated on its ability to identify *every attacker-influenced process* in each dataset.

**Comparison Baseline.** Benchmarking ORCHID’s performance on entity-level classification excludes most prior work, the majority of which does whole-graph classification [5]–[7], [9] and is particularly vulnerable to mimicry attacks [10], [11]. Even sub-graph systems like SIGL [19] and Prographer [8] still, fundamentally perform graph-level classification, but on smaller time slices. Shadewatcher [12] is the only GNN-based IDS that performs entity-level classification. Unfortunately, when we contacted the authors of

Shadewatcher, they informed us they built Shadewatcher on proprietary code that they could not release.

Instead, we evaluate ORCHID against two Graph Neural Network architecture variants. The first model, *Full-GNN*, represents a traditional offline deployment model where the model constructs the full graph (training and test data) before training begins. This model performs nearly identically to ShadeWatcher on the same dataset (Trace) that appeared in their evaluation [12]. The second model, *Stream-GNN*, attempts to adapt the Full-GNN to a streaming setting. The Stream-GNN model uses the same training data given to ORCHID in each experiment, and is also unable to pre-populate its adjacency matrix and node matrix to reflect events and entities that only appear during the test period.

Stream-GNN is thus an approximation to the discriminatory power of a GNN under ORCHID’s deployment model.

Another limitation of GNN architectures is their inability to efficiently represent lossless provenance graphs (e.g., versioned). Unsurprisingly, *attempting to train a PyTorch GNN on a versioned provenance graph quickly results in an out-of-memory error* even on a well-provisioned GPU server. Provenance graphs, even those that describe a single system, are simply much larger than the graphs used to evaluate other graph learning systems, and current architectures cannot scale. As a workaround, our baseline models use a simplified provenance representation that fails to capture the temporal ordering between events and results in *false provenance*. For example, if a process reads from file A, writes to file B, and then reads from file C, a GNN will incorrectly include file C in file B’s embedding. This is the same approach used by previous GNN-based approaches [12], [19]. A hyperparameter search revealed that 2 layers and 8 heads delivered the optimal performance for both GNNs. We trained each GNN for a maximum of 1000 epochs with early stopping, using Cross-Entropy loss and the Adam optimizer to tune the model weights.

**Streamspot Dataset.** Results for Streamspot can be found in Figure 3a. Across the entire continuum of detection thresholds, Full-GNN significantly outperforms ORCHID (0.78 vs. 0.59 AUC). Unsurprisingly, Full-GNN creates a more effective embedding model, given its ability to learn on edges after the training period. We expected Full-GNN to represent a performance ceiling for ORCHID.

However, in the critical range of detection thresholds with low FPR values, ORCHID offers several effective performance rates. ORCHID can detect 23% of all malicious entities, representing at least one detection for each attack behavior, with 0% FPR, and nearly reaches the Full-GNN’s 0% FPR detection rate while admitting just 9% FPR. On the other hand, given comparable training data (Stream-GNN), the GNN’s performance hovers around chance (0.51 AUC).

**Theia Dataset.** In Figure 3b, we see a similar trend to StreamSpot where Full-GNN outperforms ORCHID (1.00 vs. 0.91 AUC) while ORCHID outperforms Stream-GNN (0.91 AUC vs. 0.73 AUC).

Furthermore, ORCHID achieves 97% detection with 15% FPR, indicating that ORCHID can separate most of the attack within Theia from benign behavior. However, certain attack

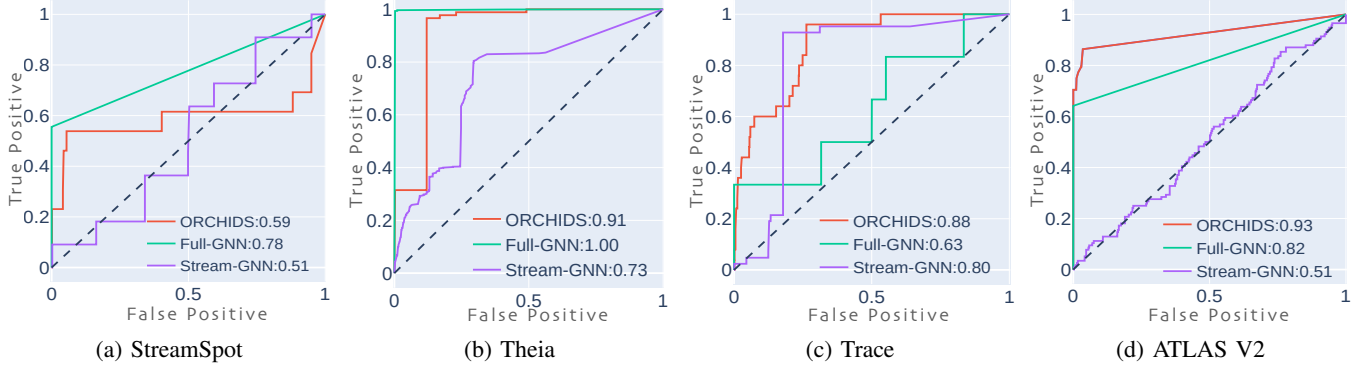


Figure 3: Performance of ORCHID, reported as ROC curves, as compared to GNN-based approaches. In a streaming setting, ORCHID’s performance is generally comparable to an offline GNN deployment (Full-GNN), particularly in the low-FPR regions of the plot that denote plausible detection thresholds. Adapting the GNN to an online setting with equivalent training data to ORCHID (Stream-GNN), the GNN model is thoroughly outperformed.

entities are more challenging to separate as they may only be tangentially related to the attack.

**Trace Dataset.** Against the much larger Trace dataset (Figure 3c), we are surprised to see that ORCHID outperforms the Full-GNN (0.88 vs 0.63 AUC). In the critical region of low FPR detection thresholds, Full-GNN offers a higher detection rate of 35% at 0% FPR, while ORCHID can offer a 60% TPR with a manageable 12% FPR. It’s difficult to say which is preferable, and both systems can detect at least one entity in each attack. Interestingly, Stream-GNN outperforms Full-GNN across the entire continuum (0.8 vs. 0.63 AUC), although its gains come at impractically high FPR values.

**ATLASv2 Dataset.** Results in Figure 3d deviate from the previous pattern. Here, ORCHID unambiguously outperforms the Full-GNN, offering superior TPR rate at 0% FPR and approaching 89% TPR at near-zero FPR. Stream-GNN’s performance again hovers at 0.51 AUC.

**Remarks.** For three out of the four datasets, ORCHID was surpassed in classification performance by Full-GNN. We expected this, given that the GNN had the advantage of learning its embedding function in a static graph that represented the entire dataset, providing more information to the model during training time. Full-GNN could overcome the distribution shifts present between the training and testing datasets, enabling it to model benign activity more accurately. Interestingly, ORCHID performed better on the ATLASv2 dataset than the Full-GNN. One potential reason for this outcome is that certain attack nodes in ATLAS were spaced out from each other, making them unable to be directly correlated within the limited  $K$ -hop neighborhood view of the Full-GNN. Conversely, ORCHID, could capture longer-term dependencies, allowing it to discern patterns that the full GNN’s local viewpoint may miss. Regardless of performance variance by dataset, both systems could detect one or more malicious entities in each attack at a low FPR threshold.

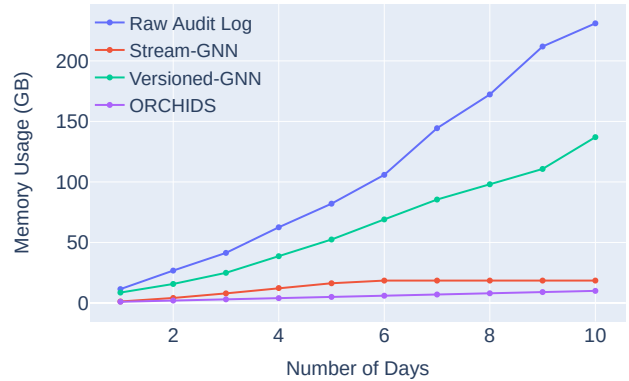


Figure 4: Memory consumption of different IDS models on the Trace dataset, as compared to the raw audit log. *Versioned-GNN* denotes the memory footprint of Full-GNN if it operated on the more precise versioned provenance graph used by ORCHID. We were only able to successfully train Full-GNN on 2 days of the versioned graph; subsequent points on this line are estimates.

#### 5.4. Performance Evaluation (RQ3)

So far, we have demonstrated that ORCHID can accurately classify malicious activity, performing similarly to an offline GNN trained on larger amounts of data. We now evaluate ORCHID runtime performance in a streaming deployment model, considering issues of resource consumption and detection latency, as compared to prior work.

**Memory Consumption.** ORCHID operates with significantly reduced memory consumption compared to previous approaches. By processing events in the graph in a streaming fashion and tracking embeddings for each system entity, ORCHID reduces the terms in its memory consumption from  $|E| + |V|$  to  $|V|$ .<sup>3</sup> The memory reduction acquired by removing the edge term  $|E|$  compounds over time as the number of system entities grows slower than the number of

3. Technically, the GNN doesn’t have an  $|E|$  term because it reserves a space for every possible edge. It is actually  $|V| * |V| + |V|$ .



Task	Model	Checkpoint Interval (Num. Edges)					V
		1	1K	100K	1M	EOF	
PP	ORCHID	-	-	-	-	28.9K	4.08M
	Stream-GNN	-	-	-	-	66.7K	1.36M
	Full-GNN	-	-	-	-	66.7K	1.36M
T	ORCHID	518K					
	Stream-GNN	62.8K					
ED	ORCHID	444K	444K	444K	444K	444K	4.08M
	Stream-GNN	160B	160M	1.60M	160K	400	1.36M
TED	Full-GNN	-	-	-	-	67.4K	1.36M

TABLE 2: Record the total runtime (in seconds) of Preprocessing (PP), Training (T), Embedding and Detection (ED) model tasks using the Trace dataset. TED reflect testing time costs and occur immediately after training for the Full-GNN. Training (T) time refers to time it takes to the constant time it takes to train the model offline. The single number we report for both models at checkpoint interval 1 is representative for the time it takes to train ORCHID or Stream-GNN across all checkpoint intervals. Checkpoint Interval reflects that variation in embedding and detection cost based on how many edges are added per test batch, with EOF indicating all edges are added at once. |V| is the total number of nodes each system encounters in its representation of the underlying graph.

system events. Intuitively, activity predominately consists of existing system entities interacting with other system entities rather than generating new system entities.

This assertion is validated within Figure 4, where we plot ORCHID’s memory consumption on increasingly larger portions of the Trace dataset. To provide context, we also plot the memory consumption of Stream- and Versioned-GNN. Stream-GNN represents the memory consumption of the GNN on an unversioned graph, ignoring the provenance graph’s temporal attributes. The memory consumption of Stream-GNN at the end of the dataset represents the memory consumption for Full-GNN. Versioned-GNN represents the memory consumption of GNN on the more precise *versioned* graph that ORCHID utilizes, requiring 143.7GB to store in memory. The difference in memory consumption between *Full-GNN* and *Versioned-GNN* underscores the reality that GNNs utilize less precise graph representations. Even with a less precise graph representation, Stream and Full-GNN maintain a higher memory footprint (10.4 GB) than ORCHID whose footprint is at most 2.7 GB while modeling the entirety of the 270 GB dataset

**Computation Cost.** We now report on the raw processing speed of each model, inspecting the runtime of three model tasks: preprocessing, training, and embedding and detection. Preprocessing indicates the time required to map the log into memory and process it into a provenance graph. Training is an upfront cost for ORCHID and Stream-GNN, but a backend cost for the Full-GNN that immediately precedes embedding and detection; therefore, it is important to note that these *runtime costs* do not yet reflect *detection latency* for ORCHID and Stream-GNN. An important performance distinction between our RNN architecture and the

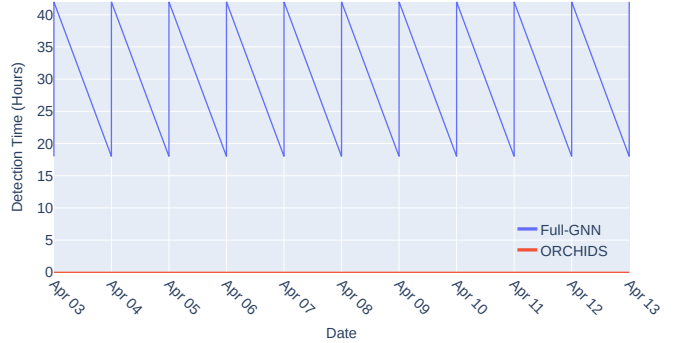


Figure 5: Detection Lag of different IDS models on the Trace dataset. Averaged from older runs, *Full-GNN* takes 6 hours to train and analyze audit log. Because of the granularity of the graph, *ORCHID* appears to have 0 lag during detection but *ORCHID* requires 0.002 seconds to process each event.

GNNs is the opportunity for parallelization; while ORCHID operates on sequential edges at a constant cost, the GNN can parallelize across portions of the static graph. To reflect this advantage for the Stream-GNN, we report embedding and detection for different *Checkpoint Intervals* of data. We report the total time for the Stream-GNN to embed and classify 1 edge at a time, 1K edges, etc., with EOF indicating the full test batch.

Results are summarized in Table 2. ORCHID has an advantage in the pre-processing stage because it does not need to generate a provenance graph, and map the edges into memory. When comparing the offline training time between ORCHID and Stream-GNN, Stream-GNN provides a better runtime as it can batch over the static provenance graph, allowing for greater parallelization. While ORCHID does not utilize batching, it is possible to batch non-dependent events together, allowing for faster training time. In comparing the embedding and detection (ED) time for ORCHID and Stream-GNN, Stream-GNN outperforms ORCHID when operating on batches of 1M edges or greater due to the GNN’s ability to parallelize computation over a known static graph. In contrast, ORCHID must operate on one large stream of sequential data.

*Without parallelization, the GNN requires 160 billion seconds to complete, a 360K times increase over ORCHID.* For the same reasons, ORCHID test time costs are independent of checkpoint intervals, processing edges at a constant rate of 300 edges per second.

**Detection Latency.** The true cost of the GNN deployment model is exposed when considering the lag between an event’s occurrence and its classification. Based on the time required to train and test the Full-GNN model on the Trace dataset (67.4K seconds, or 18 hours), consider a practical deployment model where a GNN classifier trains on the previous 14 days’ worth of data at midnight each night, then immediately attempts to classify the observed events from the previous day. Instead of re-training and detecting Full-GNN on each of the 14 days of Trace, we averaged over the

time Full-GNN took to run over the different datasets (§5.3) to estimate the average time it would take Full-GNN to train and test every night. We compare the resulting detection lag to ORCHID’s latency in its streaming embedding and detection mode.

The results are pictures in Figure 5 for the Trace dataset. The x-axis depicts the time series of Trace, while the y-axis depicts the expected detection lag for an event that occurs at that time. Depending on the time of day, ORCHID reduces detection lag by a minimum of *10 million times* up to a maximum of *43 million times* by eschewing the GNN’s offline deployment model. The minimum time detection lag for Full-GNN for an event that occurred directly right before analysis would still be 18 hours, while the maximum time for an event that occurred right after analysis occurred would be 42 hours. ORCHID, on the other hand, could process each event after it occurred, providing a detection lag time of 0.002 seconds. By streaming, ORCHID is able to considerably reduce the attacker’s “dwell” time on the system, becoming more in line with the runtime associated with commercial EDR tools [30].

## 6. Discussion

ORCHID is a streaming-based Prov-IDS that aims to provide anomaly detection in or close to real-time. However, certain limitations to its design prevent it from being a perfect solution.

**Disappearing Memory.** The efficacy of ORCHID depends on its ability to represent long provenance histories as the system evolves. Because each embedding is supposed to be a meaningful combination of all the events that brought a system entity to its present state the backbone neural network needs to be able to remember that history. However, previous work has shown that RNNs can forget certain paths as they get longer, suggesting embeddings that are output by an RNN may not reflect all edges that have gone into them. In practice, this could be weaponized by an attacker that spaces out key attack steps to break the causal links within the embedding space. ORCHID mitigates this problem by explicitly re-linking root cause entities to their distant successor entities within the embedding. This mitigation appears to be effective, given the limitations of publicly available test data. Future work may investigate solutions to boost further RNNs’ memory, such that the number of edges forgotten becomes prohibitive.

**Log Retention.** We have touted the ability of ORCHID to efficiently and accurately represent large provenance graphs for anomaly detection purposes. However, ORCHID’s representation of the audit log may not prove as useful for downstream tasks like threat hunting and attack forensics. This means that ORCHID is not a replacement for long-term retention of audit logs, which are needed to verify and respond to the threats detected by ORCHID. At present, the explainability of ORCHID classification results still depends on an analyst querying the provenance graph of the offending process and interpreting the results. While ORCHID facilitates linkability between its detections and

the audit log, we hope to integrate explainability into the detection model better in future work.

## 7. Related Works

**Streaming Provenance Anomaly Detection.** The issue of processing speed for provenance-based anomaly detection has been considered in prior work. Digest-based vectorization provides an efficient means of quickly representing large graphs for cluster analysis. Manzoor et al.’s Streamspot reports an per-edge throughput of  $70\mu s$  with a 1000 bit digest [5]. Han et al.’s Unicorn does not report per-edge throughput, but is shown to maintain roughly line speed with the underlying audit framework [6]. However, both Streamspot and Unicorn perform whole-graph/system classification, a technique that is known to be vulnerable to adversary evasion [10] due to the fact that attacks typically account for a miniscule proportion of total system activity. Wang et al.’s ProvDetector performs program classification, but does so by analyzing large system subgraphs (e.g. of depth 10) centered on the program to be classified [7]. Rather than digests, ProvDetector down-samples the graph to a small number of paths (e.g., 20) and then embeds each using a doc2vec model. In a 100 endpoint organization, the authors estimate that a corpus of 30 programs could be monitored in about 5.7 hours, indicating that their system also keeps pace with the event stream. However, by operating on larger subgraphs, their system is also more susceptible to evasion [10].<sup>4</sup> GNN-based approaches like Shadewatcher [12] are computationally efficient, but are only effective if training starts after the inference/testing events have already occurred, thus making them much slower than their event processing speed would suggest. All of the above approaches may benefit from online graph learning techniques (e.g., [31]) as a means of transitioning away from the offline classification model. In contrast, ORCHID can perform real-time processing of the event stream while maintaining a lossless representation of the provenance graph and monitoring *all* programs on the system.

**Provenance and Rule-based Intrusion Detection.** Today’s Endpoint Detection & Response (EDR) products rely primarily on rule (heuristic) intrusion detection, in which the event stream is pattern matched against a set of hand-written queries describing a known attack behavior. Recent work has observed that pattern matching approaches are also applicable for provenance graph representations of the event stream [32]–[34]. Provenance has also been used to triage/prioritize the alerts of traditional endpoint detection products [35], [36], demonstrating synergy between event sequence and provenance analysis. Because these approaches do not require training machine learning models, they do not face the same deployment challenges in streaming environments, although retaining graphs in memory becomes an issue as they grow [37].

4. An additional concern is that multi-path dependencies, e.g., fusions of data, are not possible to express in ProcDetector representations.

Sequence-based Anomaly Detection. In contrast to provenance, traditional host anomaly detection has modeled the sequences of system calls in an event stream [38]–[41]. Event sequence analysis continues to enjoy popularity today, with anomaly detectors based on neural networks [42]–[44]. Because sequence analysis only considers a highly localized window of activity, streaming applications are much more straightforward to produce. However, given that classic sequence-based anomaly detectors were shown to be susceptible to mimicry attacks [45], [46], it is not clear how the introduction of deep learning models has improved their security, if at all. It may be that analysis of higher-level event streams such as EDR [47] and NDR [48] data mitigates this problem.

Attack Reconstruction. Provenance’s original applications in security were in *attack reconstruction*, i.e., identifying the steps of an attack once some indicator of compromise had already been discovered. Work in this area includes, ATLAS a supervised approach to search for attack sequences in a provenance graph using prior knowledge of attacker behaviors [49]. WATSON clusters provenance subgraphs into higher-level abstract behaviors, which can then be used to help analysts understand attacker behaviors [50]. Similarly, DepComm reduces provenance graphs into communities, or smaller subgraphs, that represent some particular behavior [51]. UIScope additionally integrates application-layer UI events to understand behaviors [52]. Improvements to intrusion detection algorithms significantly simplify attack reconstruction by offering more precise and reliable indicators of compromise, as provided by ORCHID. In turn, attack reconstruction systems can aid ORCHID by identifying the minority of processes in the attack chain that were not initially detected.

## 8. Conclusion

We introduce ORCHID, a streaming Prov-IDS capable of fine-grained entity-level classification. ORCHID produces node embeddings that account for all edge relationships in a provenance graph at a fraction of the memory cost. We show these embeddings achieve competitive anomaly detection results with state-of-the-art prov-HIDS systems.

## References

- [1] R. Huber, “Syscall auditing at scale,” Slack Engineering Blog, 2017. [Online]. Available: <https://slack.engineering/syscall-auditing-at-scale/>
- [2] Microsoft, “Sysmon v15.0,” <https://learn.microsoft.com/en-us/sysinternals/downloads/sysmon>, 2023.
- [3] VM Ware, “VMware Carbon Black EDR Documentation,” <https://docs.vmware.com/en/VMware-Carbon-Black-EDR/index.html>, 2023.
- [4] Red Hat, “Configure Linux system auditing with auditd,” <https://www.redhat.com/sysadmin/configure-linux-auditing-auditd>, 2023.
- [5] E. Manzoor, S. M. Milajerdi, and L. Akoglu, “Fast memory-efficient anomaly detection in streaming heterogeneous graphs,” in *Proceedings of the 22nd ACM SIGKDD International Conference on Knowledge Discovery and Data Mining*, ser. KDD ’16. New York, NY, USA: Association for Computing Machinery, 2016, pp. 1035–1044. [Online]. Available: <https://doi.org/10.1145/2939672.2939783>

- [6] X. Han, T. Pasqueir, A. Bates, J. Mickens, and M. Seltzer, “ Unicorn: Runtime Provenance-Based Detector for Advanced Persistent Threats,” in *27th ISOC Network and Distributed System Security Symposium*, ser. NDSS’20, February 2020.
- [7] Q. Wang, W. U. Hassan, D. Li, K. Jee, X. Yu, K. Zou, J. Rhee, Z. Zhen, W. Cheng, C. A. Gunter, and H. chen, “You Are What You Do: Hunting Stealthy Malware via Data Provenance Analysis,” in *27th ISOC Network and Distributed System Security Symposium*, ser. NDSS’20, February 2020.
- [8] F. Yang, J. Xu, C. Xiong, Z. Li, and K. Zhang, “Prographer: An anomaly detection system based on provenance graph embedding.”
- [9] Y. Xie, D. Feng, Y. Hu, Y. Li, S. Sample, and D. Long, “Pagoda: A hybrid approach to enable efficient real-time provenance based intrusion detection in big data environments,” *IEEE Transactions on Dependable and Secure Computing*, vol. 17, no. 6, pp. 1283–1296, 2018.
- [10] A. Goyal, X. Han, A. Bates, and G. Wang, “Sometimes, You Aren’t What You Do: Mimicry Attacks against Provenance Graph Host Intrusion Detection Systems,” in *30th ISOC Network and Distributed System Security Symposium*, ser. NDSS’23, February 2023.
- [11] K. Mukherjee, J. Wiedemeier, T. Wang, J. Wei, F. Chen, M. Kim, M. Kantarcioglu, and K. Jee, “Evading provenance-based ml detectors with adversarial system actions,” in *Proceedings of USENIX Security Symposium (SEC)*, ser. USENIX ’23, 2023.
- [12] J. Zengy, X. Wang, J. Liu, Y. Chen, Z. Liang, T.-S. Chua, and Z. L. Chua, “Shadewatcher: Recommendation-guided cyber threat analysis using system audit records,” in *2022 IEEE Symposium on Security and Privacy (SP)*. IEEE, 2022, pp. 489–506.
- [13] A. D. Keromytis, “Darpa transparent computing,” <https://github.com/darpa-i2o/Transparent-Computing>, 2018.
- [14] Groth, Paul and Moreau, Luke, “Prov-overview: an overview of the prov family of documents,” 2013.
- [15] K.-K. Muniswamy-Reddy, D. A. Holland, U. Braun, and M. Seltzer, “Provenance-aware Storage Systems,” in *Proceedings of the Annual Conference on USENIX ’06 Annual Technical Conference*, ser. Proceedings of the 2006 Conference on USENIX Annual Technical Conference, Jun. 2006.
- [16] A. Goyal, G. Wang, and A. Bates, “R-CAID: Embedding Root Cause Analysis within Provenance-based Intrusion Detection,” in *2024 IEEE Symposium on Security and Privacy*, may 2024.
- [17] S. Ma, J. Zhai, Y. Kwon, K. H. Lee, X. Zhang, G. Ciocarlie, A. Gehani, V. Yegneswaran, D. Xu, and S. Jha, “Kernel-supported cost-effective audit logging for causality tracking,” in *2018 USENIX Annual Technical Conference (USENIX ATC 18)*. Boston, MA: USENIX Association, 2018, pp. 241–254. [Online]. Available: <https://www.usenix.org/conference/atc18/presentation/ma-shiqing>
- [18] Crowdstrike, “Why Dwell Time Continues to Plague Organizations,” <https://www.crowdstrike.com/blog/why-dwell-time-continues-to-plague-organizations/>, 2019.
- [19] X. Han, X. Yu, T. Pasquier, D. Li, J. Rhee, J. Mickens, M. Seltzer, and H. Chen, “SIGL: Securing software installations through deep graph learning,” in *30th USENIX Security Symposium (USENIX Security 21)*. USENIX Association, Aug. 2021, pp. 2345–2362. [Online]. Available: <https://www.usenix.org/conference/usenixsecurity21/presentation/han-xueyuan>
- [20] “MITRE ATT&CK,” <https://attack.mitre.org>, 2019.
- [21] “MITRE ATT&CK: Masquerading,” <https://attack.mitre.org/techniques/T1078>, 2020.
- [22] D. E. Rumelhart, G. E. Hinton, R. J. Williams *et al.*, “Learning internal representations by error propagation,” 1985.
- [23] Q. Le and T. Mikolov, “Distributed representations of sentences and documents,” in *International conference on machine learning*. PMLR, 2014, pp. 1188–1196.

- [24] S. Hochreiter and J. Schmidhuber, "Long short-term memory," *Neural computation*, vol. 9, no. 8, pp. 1735–1780, 1997.
- [25] A. Alsaheel, Y. Nan, S. Ma, L. Yu, G. Walkup, Z. B. Celik, X. Zhang, and D. Xu, "ATLAS: A sequence-based learning approach for attack investigation," in *30th USENIX Security Symposium (USENIX Security 21)*. USENIX Association, Aug. 2021, pp. 3005–3022. [Online]. Available: <https://www.usenix.org/conference/usenixsecurity21/presentation/alsaheel>
- [26] A. Riddle and K. Westfall, "Atlas v2: An open-source dataset for intrusion detection research," <https://bitbucket.org/sts-lab/atlasv2/>.
- [27] J. Liu, A. Inam, A. Goyal, K. Westfall, A. Riddle, and A. Bates, "Reapr: Recovery every attack process," <https://bitbucket.org/sts-lab/reapr-ground-truth>, 2023.
- [28] K. Cho, B. Van Merriënboer, C. Gulcehre, D. Bahdanau, F. Bougares, H. Schwenk, and Y. Bengio, "Learning phrase representations using rnn encoder-decoder for statistical machine translation," *arXiv preprint arXiv:1406.1078*, 2014.
- [29] N. Carlini, D. Ippolito, M. Jagielski, K. Lee, F. Tramèr, and C. Zhang, "Quantifying memorization across neural language models," *arXiv preprint arXiv:2202.07646*, 2022.
- [30] "Endpoint Detection and Response Solutions Market," <https://www.gartner.com/reviews/market/endpoint-detection-and-response-solutions>, 2019.
- [31] R. Trivedi, M. Farajtabar, P. Biswal, and H. Zha, "Dyrep: Learning representations over dynamic graphs," in *International conference on learning representations*, 2019.
- [32] S. M. Milajerdi, R. Gjomemo, B. Eshete, R. Sekar, and V. Venkatakrishnan, "Holmes: real-time apt detection through correlation of suspicious information flows," in *2019 IEEE Symposium on Security and Privacy (SP)*. IEEE, 2019, pp. 1137–1152.
- [33] S. M. Milajerdi, B. Eshete, R. Gjomemo, and V. N. Venkatakrishnan, "Propatrol: Attack investigation via extracted high-level tasks," in *Information Systems Security*, V. Ganapathy, T. Jaeger, and R. Shyam-sundar, Eds. Cham: Springer International Publishing, 2018, pp. 107–126.
- [34] M. N. Hossain, S. M. Milajerdi, J. Wang, B. Eshete, R. Gjomemo, R. Sekar, S. Stoller, and V. Venkatakrishnan, "SLEUTH: Real-time attack scenario reconstruction from COTS audit data," in *26th USENIX Security Symposium (USENIX Security 17)*. Vancouver, BC: USENIX Association, 2017, pp. 487–504. [Online]. Available: <https://www.usenix.org/conference/usenixsecurity17/technical-sessions/presentation/hossain>
- [35] W. U. Hassan, S. Guo, D. Li, Z. Chen, K. Jee, Z. Li, and A. Bates, "Nodoze: Combatting threat alert fatigue with automated provenance triage," in *network and distributed systems security symposium*, 2019.
- [36] W. U. Hassan, A. Bates, and D. Marino, "Tactical provenance analysis for endpoint detection and response systems," in *2020 IEEE Symposium on Security and Privacy (SP)*. IEEE, 2020, pp. 1172–1189.
- [37] W. U. Hassan, D. Li, K. Jee, X. Yu, K. Zou, D. Wang, Z. Chen, Z. Li, J. Rhee, J. Gui, and A. Bates, "This is why we can't cache nice things: Lightning-fast threat hunting using suspicion-based hierarchical storage," in *Annual Computer Security Applications Conference*, ser. ACSAC '20. New York, NY, USA: Association for Computing Machinery, Dec 2020, pp. 165–178. [Online]. Available: <https://doi.org/10.1145/3427228.3427255>
- [38] S. Forrest, S. A. Hofmeyr, A. Somayaji, and T. A. Longstaff, "A sense of self for unix processes," in *Proceedings of the 1996 IEEE symposium on security and privacy*. IEEE, 1996, pp. 120–128.
- [39] S. A. Hofmeyr, S. Forrest, and A. Somayaji, "Intrusion detection using sequences of system calls," *Journal of computer security*, vol. 6, no. 3, pp. 151–180, 1998.
- [40] W. Lee and S. Stolfo, "Data mining approaches for intrusion detection," 1998.
- [41] R. Sekar, M. Bendre, D. Dhurjati, and P. Bollineni, "A fast automaton-based method for detecting anomalous program behaviors," in *Proceedings 2001 IEEE Symposium on Security and Privacy. S&P 2001*. IEEE, 2000, pp. 144–155.
- [42] M. Du, F. Li, G. Zheng, and V. Srikumar, "Deeplog: Anomaly detection and diagnosis from system logs through deep learning," in *Proceedings of the 2017 ACM SIGSAC conference on computer and communications security*, 2017, pp. 1285–1298.
- [43] W. Meng, Y. Liu, Y. Zhu, S. Zhang, D. Pei, Y. Liu, Y. Chen, R. Zhang, S. Tao, P. Sun *et al.*, "Loganomaly: Unsupervised detection of sequential and quantitative anomalies in unstructured logs," in *IJCAI*, vol. 19, no. 7, 2019, pp. 4739–4745.
- [44] S. Nedelkoski, J. Bogatinovski, A. Acker, J. Cardoso, and O. Kao, "Self-attentive classification-based anomaly detection in unstructured logs," in *2020 IEEE International Conference on Data Mining (ICDM)*. IEEE, 2020, pp. 1196–1201.
- [45] D. Wagner and P. Soto, "Mimicry attacks on host-based intrusion detection systems," in *Proceedings of the 9th ACM Conference on Computer and Communications Security*, 2002, pp. 255–264.
- [46] K. M. Tan and R. A. Maxion, "'why 6?'" defining the operational limits of stide, an anomaly-based intrusion detector," in *Proceedings of the 2002 IEEE Symposium on Security and Privacy*. IEEE, 2002, pp. 188–201.
- [47] Y. Shen, E. Mariconti, P. A. Vervier, and G. Stringhini, "Tiresias: Predicting security events through deep learning," in *Proceedings of the 2018 ACM SIGSAC Conference on Computer and Communications Security*, ser. CCS '18. New York, NY, USA: Association for Computing Machinery, 2018, pp. 592–605. [Online]. Available: <https://doi.org/10.1145/3243734.3243811>
- [48] T. v. Ede, H. Aghakhani, N. Spahn, R. Bortolameotti, M. Cova, A. Continella, M. v. Steen, A. Peter, C. Kruegel, and G. Vigna, "Deepcase: Semi-supervised contextual analysis of security events," in *2022 IEEE Symposium on Security and Privacy (SP)*, 2022, pp. 522–539.
- [49] A. Alsaheel, Y. Nan, S. Ma, L. Yu, G. Walkup, Z. B. Celik, X. Zhang, and D. Xu, "Atlas: A sequence-based learning approach for attack investigation," in *USENIX Security Symposium*, 2021, pp. 3005–3022.
- [50] J. Zeng, Z. L. Chua, Y. Chen, K. Ji, Z. Liang, and J. Mao, "Watson: Abstracting behaviors from audit logs via aggregation of contextual semantics," in *NDSS*, 2021.
- [51] Z. Xu, P. Fang, C. Liu, X. Xiao, Y. Wen, and D. Meng, "Depcomm: Graph summarization on system audit logs for attack investigation," in *2022 IEEE Symposium on Security and Privacy (SP)*. IEEE, 2022, pp. 540–557.
- [52] R. Yang, S. Ma, H. Xu, X. Zhang, and Y. Chen, "Uiscope: Accurate, instrumentation-free, and visible attack investigation for gui applications," in *NDSS*, 2020.

## Appendix

### 1. Streaming Classification Over Time

Like any learning system, ORCHID must contend with the possibility of concept drift or the shift in distribution between the real world and the data the model was trained on. For host systems, concept drift can be reflected by changes in workloads, where the model of normality used by the IDS to detect abnormal behavior is no long representative of the users behavior. As a result, the abnormality of the user's normal behavior increases leading to higher number of false alerts outputted by the system. Evaluating the effects of concept drift on the performance of the IDS is not easy

#### Audit Log

1. Fluxbox exec firefox 1-3
2. Firefox 1 writes to ~/.cache/\*
3. Firefox 2 writes to ~/.cache/\*
4. Firefox 3 clones Firefox 4
5. Firefox 4 sends to x.x.x.x
6. Firefox 1 reads from ~/.cache/\*
7. Firefox 4 recv from x.x.x.x
8. Firefox 3 recv from x.x.x.x

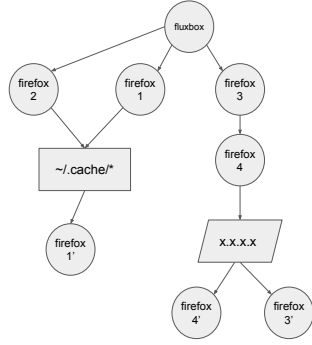


Figure 6: Visualization of a sample audit log and the representative provenance graph from the StreamSpot dataset. The audit log describes an the system interacting with Firefox - specifically the user visiting a website using Firefox. The audit log is ordered by time with each line indicating an additional time step.

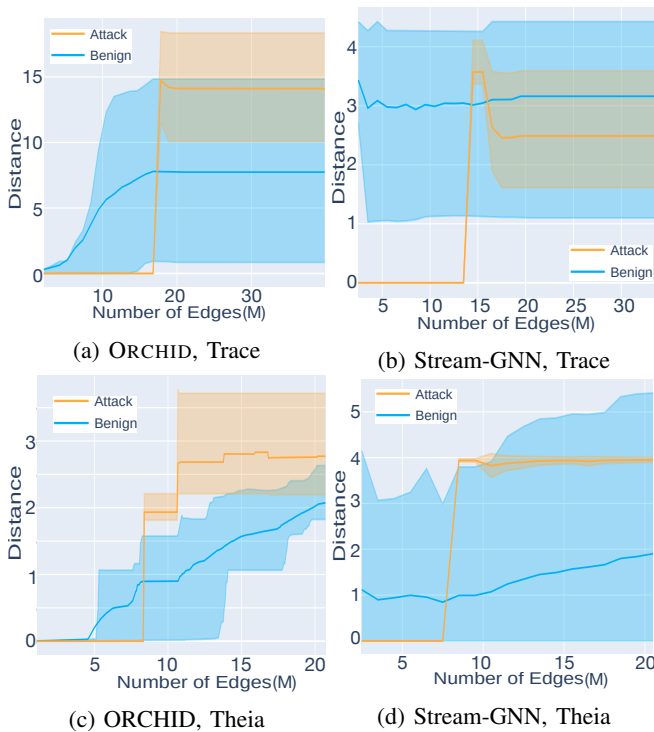


Figure 7: Distribution of nearest neighbor distance between test nodes and benign nodes at increasing time interval. The bottom line is the 25% quartile, the middle line is the mean, and the top line is the 75% quartile.

however, as as modern public intrusion detection datasets only span several days, limiting their ability to be used to exhaustively explore distribution shifts. Moreover, previous work in this area did not examine the effects of concept drift as their training data was representative of underlying distribution that was encountered at test time. To evaluate the effects of concept drift on ORCHID, we temporally reduce the size of the training dataset such that it represents only

a subset of the behaviors present within the entire dataset; thereby inducing a distribution change between the training and testing set. DARPA Transparent Computing E3 datasets, Theia and Trace represent our longest datasets lasting over 10 days. ORCHID is trained on only a single days worth of data, and evaluated over the rest of the dataset.

Figure 7 reports the mean, and upper-lower quartile for the anomaly scores of benign and attack nodes over the dataset. We report the results of both ORCHID and Stream-GNN to compare the effects of concept drift on ORCHID against previous work. Like any learning system, Figure 7 confirms ORCHID susceptibility to concept drift represented by the increase in the overall abnormality of the benign data as time progresses. For the Trace dataset (Figs. 7a-7b), the increase in abnormality for benign data stabilizes for both models.<sup>5</sup> For the Theia dataset (Fig 7c), however, ORCHID’ benign anomaly score keeps creeping up over the course of the time series. While the mean benign score still falls outside of the attack score’s confidence interval, the general trend is concerning. Understanding the disparity between these two datasets requires discussing DARPA Transparent Computing Engagement 3. During the engagement, both performers generated background (benign) activity using a periodically-executing workload script. However, the Theia performers experienced several technical issues that led to machine downtime over the course of the engagement. Examining the dataset, we believe that the Theia performers also updated their workload script during each period of downtime. As a result, the background activity in Theia represents three distributions of behavior over the course of the engagement, only one of which appeared in ORCHID’ preliminary training period. Thus, while Trace heavily advantages the models with its mono-distributional background activity, Theia inadvertently provides a small test of conceptual drift. While it’s difficult to say how similar these script changes were to naturalistic drift in machine interactions, given the available data we can at least assert that ORCHID continues to effectively classify threats over the course of a 10 day period, at which point retraining may be required.

Consistent with our classification results for this dataset, the confidence intervals of the attack distance scores indicate that ORCHID has significantly more discriminative power than Stream-GNN. Moreover the effects of concept drift on Stream-GNN are more pronounced where the upper quartile abnormality score of the benign data surpassed the upper quartile abnormality score of the attack nodes. The difference in robustness to concept drift between Stream-GNN and ORCHID can attributed to how each system processes the graph. Stream-GNN considers each node neighborhood in isolation and therefore cannot adapt to great changes to that neighborhood. Meanwhile, ORCHID learns to efficiently aggregate incoming information to existing node representations allowing for it to adapt to changes in distribution.

5. The spikes in the attack line in these plots mark the beginning of the first attack in the time series.